

This paper proposes an improved current sensing technique for a four-phase buck converter. The proposed technique is based on the conventional parallel voltage sensing with resistor-capacitor (RC) circuit. This technique requires a voltage sensor to be placed in parallel to the phase inductor. In this way, an inductor voltage which consists of high-frequency harmonics is obtained. By using RC circuit, the inductor voltage can be converted into the phase inductor current which is a requirement for the balancing current controller in a four-phase buck converter. The salient points of the proposed sensing technique are no external RC circuit is required, improving the efficiency of the converter and can be used for integrated circuit (IC) in which the conventional RC technique is not capable of. The proposed system is designed using MATLAB/SIMULINK simulation software and verified by a laboratory prototype with a TMS320F28335 as the main controller. The comparison is carried out between the proposed digital RC sensing, the conventional RC filtering sensing and series current sensing technique. Simulation and experimental results are provided to validate the system performance.

Keywords: Multiphase Converter; Series Current Sensing; Parallel Voltage Sensing; Renewable Energy.

1. Introduction

A buck-boost converter is vital in a power storage system for charging and discharging purposes. Many configurations of buck-boost converters had been introduced e.g. multiphase topology. A multiphase converter is preferred as it allows the use of smaller rated devices for a high-current application. Multiphase converter is a switch-mode power supply in which consists of power transistors, inductor, capacitor, and a diode. Its main function is to regulate the output and offers many advantages under interleaved operation [1-3]. Due to the parallel-connected structure of a multiphase converter, balancing current control is required to ensure equal current distribution among phases [4-7].

Conventionally, the series current-sensing requires a small resistor to be placed in series with the phase inductor [8]. The voltage drop across the small resistor is then fed into an integrated circuit (IC) chip in which will determine the current across the inductor. Although the series current sensing is easy to implement and does not require any additional components, however, it reduces the system's efficiency as the small resistor produces I^2R losses. To solve the issue of I^2R losses, numerous sensing techniques had been proposed. Among the proposed techniques are using the ON-resistance of a power transistor [9-10], the

* Corresponding author: Jabbar A.F., Yahaya, Universiti Tun Hussein Onn Malaysia, 86400 Parit Raja, Johor Darul Takzim, Malaysia, E-mail: jabbar@uthm.edu.my

¹ Fakulti Kejuruteraan Elektrik dan Elektronik, Universiti Tun Hussein Onn Malaysia

^{2,3} Department of EEE & IPE, Universiti Tenaga Nasional, Malaysia

⁴ Department of Computer Engineering and Computer Science, Manipal International University, Malaysia

use of resistor-capacitor (RC) circuit [11-12], and the average current sensing technique [12-13].

Among the above-mentioned current-less sensing techniques, ON-resistance has the lowest accuracy since it varies across different temperatures. The ON-resistance technique is not suitable for critical sensing purposes or used for portable appliances where the surrounding temperature changes constantly. However, it is widely used due to its lossless measuring characteristic, does not require additional components and suitable for simple sensing applications such as over-current protection, overload protection etc. The average current sensing technique produces a more accurate result and is used primarily in current control devices. This method requires additional components such as resistor (R) and capacitor (C) which are connected to the power transistor. However, this technique produces only the average current. Hence, this technique is limited to a DC-DC converter which employs average current technique as the control strategy. Other than the above-mentioned current-less sensing techniques, the parallel RC filter can be used as an alternate solution. This technique requires additional RC components and is connected in parallel to the inductor. However, the selection of RC values is based on $L / R_{DCR} = C_M R_M$. Here, C_M and R_M represent the sensing capacitor and sensing resistor. The knowledge of inductor (L) and R_{DCR} is crucial for this type of current sensing technique. One of the issues with this technique is that it is not suitable for an integrated circuit. Unlike average current-sensing, the selection of RC values and required tolerance for the integrated circuit can be complicated.

This paper proposes a current-less sensing using a digital filter to replace the use of conventional sensing technique in which show some limitations [14-15].

A voltage sensor is connected in parallel to the phase inductor and fed into the pins of analog to digital conversion (ADC) of a digital signal processor (DSP). The DSP will convert the sampling voltage into a phase inductor current. The proposed technique shows some advantages; only one voltage sensor is required without any external circuit and improved resolution in which the conventional RC sensing technique is not capable of [12]. Simulation and hardware prototype are established to verify the functions of the proposed technique. In this paper, comparison is carried out between the proposed technique, the conventional RC technique and series current sensing.

2. Notation

The notation used throughout the paper is stated below.

Indexes:

IC	integrated circuit
P_R	power losses
RC	resistor-capacitor
R_{DCR}	inductor dc-resistance

Constants:

C_M	sensing capacitor
R_M	sensing resistor
DC	direct current
L	inductance
ADC	analog to digital conversion
DSP	digital signal processor
C	capacitor

Z^T total impedance

3. Configuration and Operating Principle

3.1. Objective function

Fig. 1(i) shows the series current sensing while Fig. 1(ii) shows the conventional RC technique used in a multiphase converter. The configuration in Fig. 1(i) requires a small resistor R_s in which contributes to I^2R losses while configuration in Fig. 1(ii) requires additional passive components and is limited for application on integrated circuits.

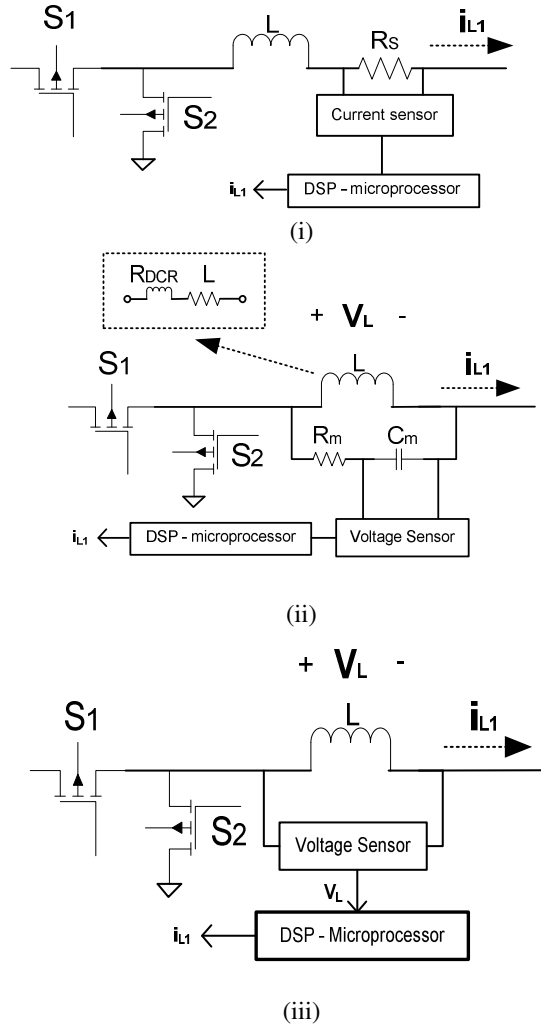


Fig. 1. (i) Series current sensing (ii) Conventional RC current sensing (iii) Proposed current-less technique

Fig. 1(iii) shows the proposed current-less technique which comprises a voltage sensor connected in parallel to the inductor (L). The measured voltage across the inductor consists of a high-frequency harmonics is fed into the DSP. With the help of a digital filter within the DSP microprocessor, the high-frequency harmonics can be converted into the equivalent current values. To fully understand the operating principle, the mathematical relationship between inductor V_L and inductor i_L must be derived. Derivation of digital filter network is based on Fig. 1(ii). According to Ohm's law, the mathematical relationship between inductor voltage V_L , and inductor current i_L is as follow:

$$V_L = L \frac{di_L}{dt} \tag{1}$$

Adding the inductor DC-Resistance (R_{DCR}) into the equation:

$$\begin{aligned} V_L &= L \frac{di_L}{dt} + (R_{DCR} \times i_L) \\ V_L &= (L \frac{d}{dt} + R_{DCR}) \times i_L \\ V_L &= (SL + R_{DCR}) \times i_L \\ V_L &= (S \frac{L}{R_{DCR}} + 1) \times i_L \end{aligned} \tag{2}$$

To see the relationship between the inductor current i_L and the filtering capacitor C_M , the voltage across the filtering capacitor must be derived. The total impedance Z_T between phase inductor L filtering components R_M and C_M is:

$$Z_T = \frac{(1/SC_m + R_m) \times (SL + R_{DCR})}{1/SC_m + R_m + SL + R_{DCR}} \tag{3}$$

Given that phase inductor V_L is also equal to

$$V_L = I_T \times Z_T \tag{4}$$

The total phase current I_T is

$$I_T = V_L \times \frac{1/SC_m + R_m + SL + R_{DCR}}{(1/SC_m + R_m) \times (SL + R_{DCR})} \tag{5}$$

Given that

$$I_T = I_F + i_L \tag{6}$$

The current across the filtering components I_F is

$$I_F = I_T \times \frac{SL + R_{DCR}}{1/SC_m + R_m + SL + R_{DCR}} \tag{7}$$

$$I_F = V_L \times \frac{SC_m}{SC_m R_m + 1}$$

The voltage across filtering capacitor can now be derived as

$$\begin{aligned}
 V_C &= I_F \times \frac{1}{SC_m} \\
 V_C &= V_L \times \frac{SC_m}{SC_m R_m + 1} \times \frac{1}{SC_m} \\
 V_C &= V_L \times \frac{1}{SC_m R_m + 1}
 \end{aligned} \tag{8}$$

From Eq. (8), it is observed that by feeding the inductor voltage V_L into the single-pole transfer function which consists of resistor-capacitor, the equivalent filtering capacitor voltage V_C is obtained. The algorithm representing a digital filter network can be taken from Eq. (8). Once the filtering capacitor voltage V_C is obtained, the inductor current i_L will also be obtained, since $V_C = i_L$. The sensing capacitor voltage is equivalent to inductor current if the values of sensing capacitors and resistors are selected such that $L/R_{DCR} = C_m R_m$. This is proven using the mathematical relationship derived as follows:

The inductor voltage previously derived in Eq. (2) is

$$V_L = \left(S \frac{L}{R_{DCR}} + 1 \right) \times i_L$$

By combining both Eq. (2) and Eq. (8), the voltage V_C across the filtering capacitor C_m is

$$V_C = \frac{S(L/R_{DCR}) + 1}{S(C_m R_m) + 1} \times i_L \tag{9}$$

From Eq. (9), if the values are selected such that $L/R_{DCR} = C_m R_m$, Eq. (9) can be further simplified into

$$V_C = i_L \tag{10}$$

From Eq. (10), it is proven that the sensing capacitor voltage V_c is equivalent to the inductor current i_L .

4. Simulation for Current-less Sensing Technique

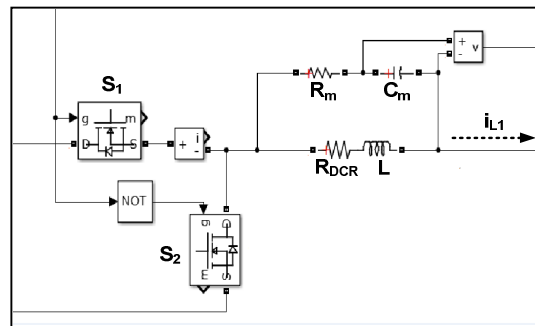
Table 1 shows the specification used for a four-phase converter. The 500W converter is tested using MATLAB/SIMULINK. The converter will be tested under two step changes:

- i. Step load from 0 to 2A
- ii. Step load from 2A to 5A

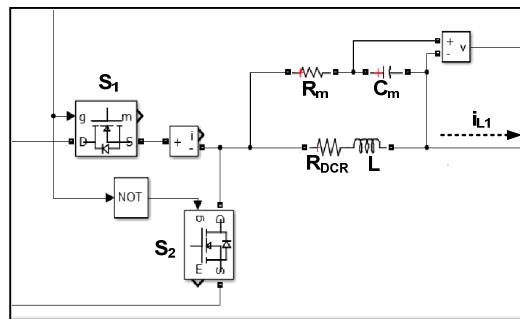
Table 1: Converter specifications

Four-phase converter	
Input Voltage (Vs)	100volts
Switching Frequency (Fs)	14kHz
Output Capacitor (C)	33uF
Inductor per Phase (L)	1mH
Inductor DC-Resistance (R _{DCR})	1Ω
Battery /Internal Resistance	48Volts / 0.048 Ω

The proposed technique is shown in Fig. 2(i) while the conventional RC technique is shown in Fig. 2(ii). The proposed technique requires only a voltage sensor as compared to the conventional RC technique. The proposed technique is shown in Fig. 2(i) while the conventional RC technique is shown in Fig. 2(ii). The proposed technique requires only a voltage sensor as compared to the conventional RC technique. The Eq. (8) seen in Fig. 2(i) represents the single pole transfer function and should be placed in the DSP for hardware implementation. For the conventional RC technique, a sensing resistor of 1kΩ and a sensing capacitor of 1μF will be used in the simulation.



(i)



(ii)

Fig. 2. Simulation setup for parallel voltage sensing:
 (i) Proposed method (ii) Conventional method $R_m = 1k\Omega$, $C_m = 1\mu F$.

Fig. 3 shows the comparison between the current sensor values, conventional RC technique and the proposed technique. The measured phase inductor voltage is shown in Fig. 3(iv).

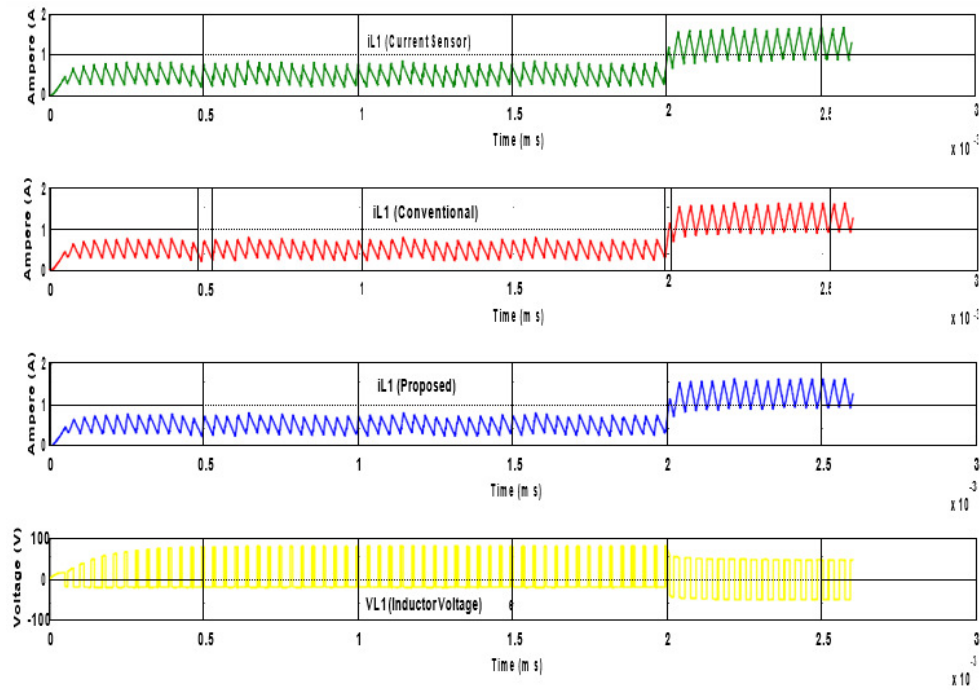


Fig. 3. Simulation results for inductor L_1 :

- (i) Measured using current sensor (ii) Conventional RC measurement technique (iii) Proposed technique (iv) Inductor voltage V_{L1} .

The result shows that the proposed technique is able to measure the inductor current i_{L1} and is similar as compared using a current sensor as per Fig. 3(i) and the conventional RC technique in Fig. 3(ii). The proposed techniques, despite measuring the signal indirectly and requires a digital filter, shows no delay in measuring the current as compared to other techniques. Fig. 3(iv) shows the measured phase inductor voltage on L_1 . The result shows that the inductor voltage consists of high-frequency pulses with respect to the input voltage V_s .

5. Experimental results

The laboratory prototype is developed for a four-phase converter using TMS320F28335 as shown in Fig. 4 and Fig. 5. The parameter used are as follows; input voltage $V_s = 100V$, inductor $L = 1mH$, filter capacitor $C = 33\mu F$, inductor DC-Resistance $R_{DCR} = 0.2\Omega$, IGBT switch IRG4PC50UD, voltage/current sensor LV25-P/LA25-NP and a 48V lithium- ion battery.

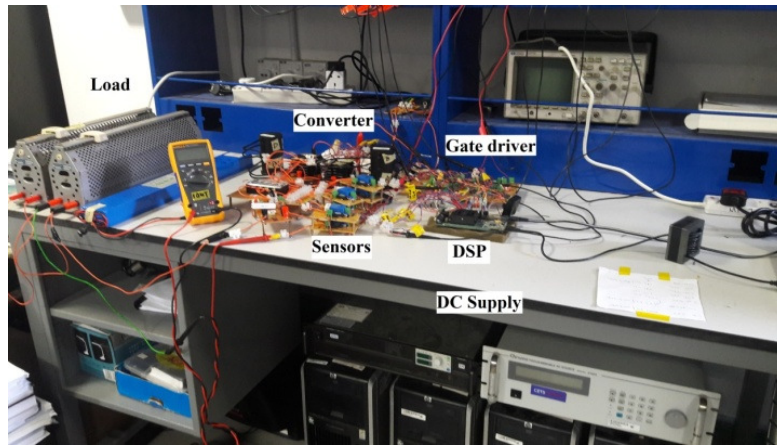


Fig. 4. Experimental setup.

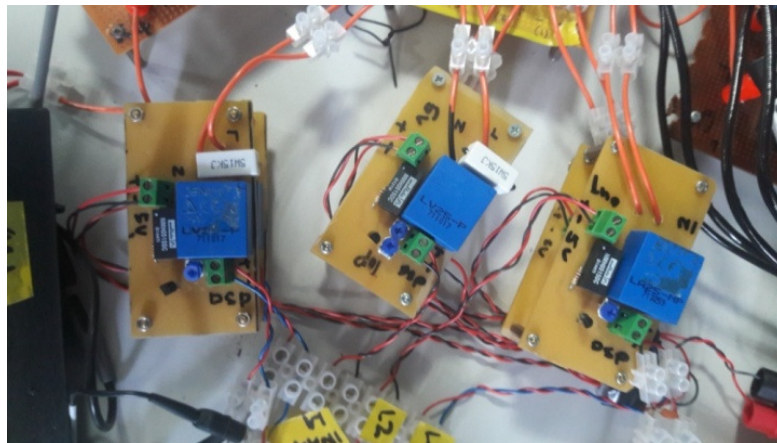


Fig. 5. Voltage and current sensor.

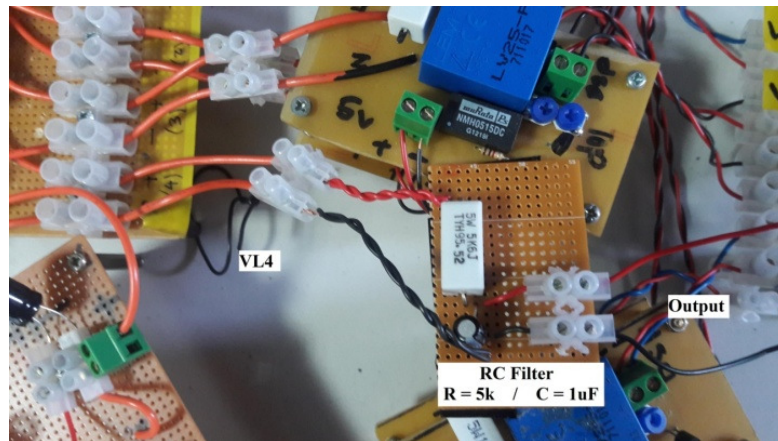


Fig. 6. Conventional RC filter ($R = 5k\Omega$, $C = 1\mu F$).

Fig. 7 shows the circuit configuration of a four-phase converter. From Fig. 7, the information of the inductor voltage V_{L1} , V_{L2} , V_{L3} , and V_{L4} will be fed into the ADC pins of the DSP. By using the proposed technique, this information can be converted into the phase inductor current i_{L1} , i_{L2} , i_{L3} , and i_{L4} . Thus, the control algorithm in the DSP will ensure equal current distribution between the inductors and regulate the battery load.

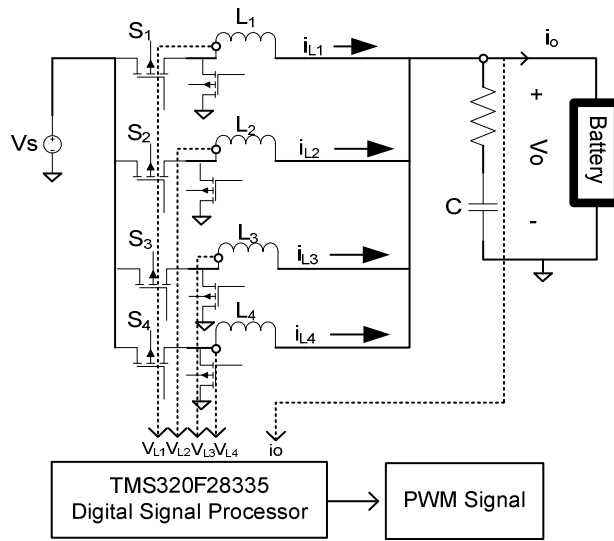


Fig. 7. Circuit configuration for the four-phase converter.

5.1 Programming setup.

From the simulation setup as per Fig. 2(i), the voltage signals are fed into a transfer function block in return produces the equivalent current values. However, in a hardware implementation, the s-transform cannot be realized directly using a coding form into the DSP microprocessor. To implement the digital filter network into the DSP microprocessor, the required transfer function (T_F) must be transformed into a state-space equation. For example,

$$T_F = \frac{1}{1 + 1.2^{-3}S} \Rightarrow \dot{x} = -833.3333(x_1) + u(t) \quad (11)$$

$$y = 833.3333(x_1)$$

From Eq. (11), the block diagram realization can be arranged as seen in Fig. 8(i). By using the arranged algorithm as per Fig. 8(i), the proposed current-less sensing can now be implemented on a DSP platform by using the code composer studio (CCS) compiler. Fig. 8(ii) shows the flow chart of the proposed technique.

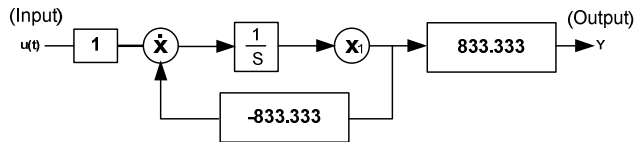


Fig. 8. Block diagram model of proposed technique.

By using the block diagram as shown in Fig. 8, the proposed technique can now be implemented on a DSP platform by using the code composer studio. Fig. 9 shows the flow chart of the algorithm.

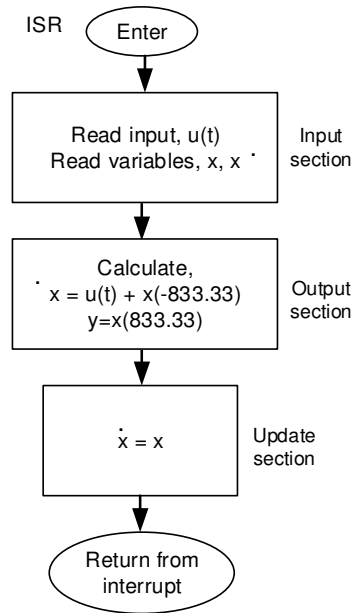


Fig. 9. Flow chart algorithm for proposed method.

5.2 Hardware results

In this experiment, the comparison between the proposed technique, the conventional RC technique, and series current sensing are conducted. Fig. 10 shows the measured analog signals from the phase inductor L_4 of all sensing techniques.

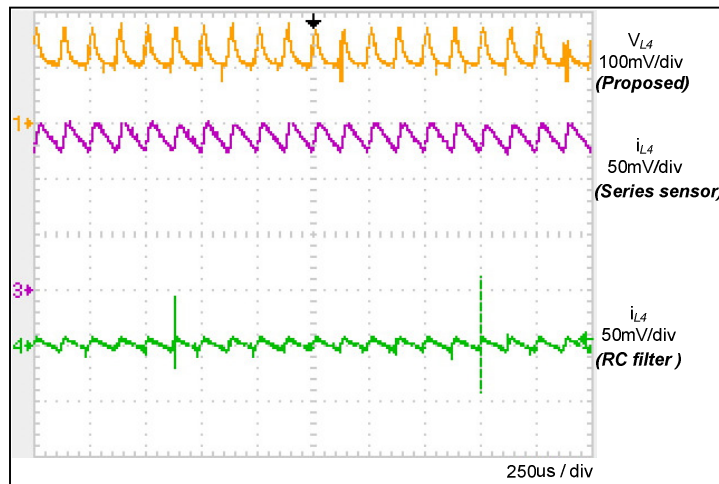


Fig. 10. Measured signals from inductor L_4 .

As can be seen from Fig. 10, the phase inductor voltage V_{L4} (orange colour) consists of high-frequency pulses with respect to the input voltage. The series current sensing (purple colour) is seen in the figure. For the conventional RC filter technique, the output of the external circuit (in Fig. 6) will produce the inductor current waveform (green colour) seen in Figure above. Figure 10 also shows that the signals of series current sensing and parallel RC sensing are similar since both of the signals represent the phase inductor current i_{L4} . These signals will be fed into the ADC pins for signal processing. An array with 40 points coordinate is placed in the 142 kHz analog to digital conversion (ADC) interrupt subroutine. For every sampling made in the ADC , the measured voltage and current will be stored in its own designated array. These arrays will be used to visualize the measured signals done by the DSP controller. Fig. 11 shows the captured digital signal of phase inductor current i_{L4} . This signal is captured using code composer studio (CCS) to visualize the analog signal in the digital world. The recorded arrays of data will be plot using $MATLAB$ for presentation.

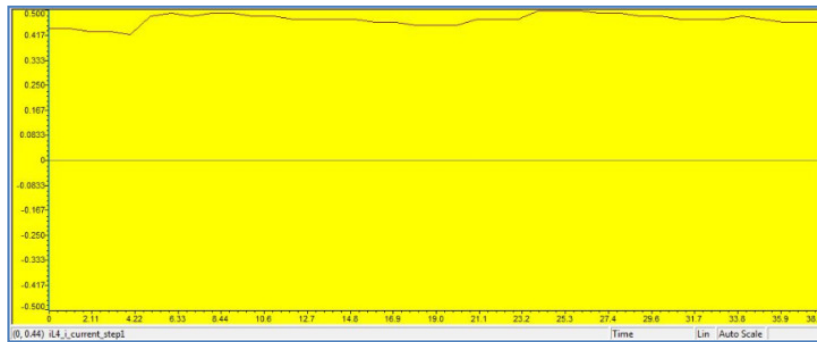
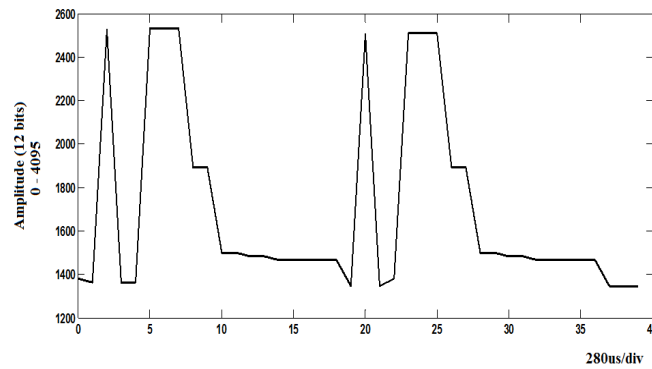
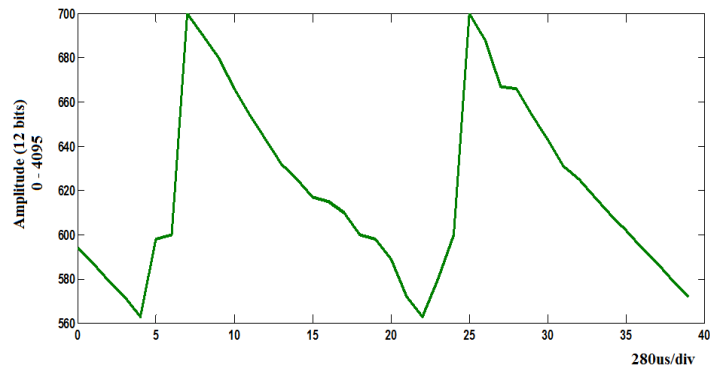


Fig. 11. Hardware results of phase inductor i_{L4} .

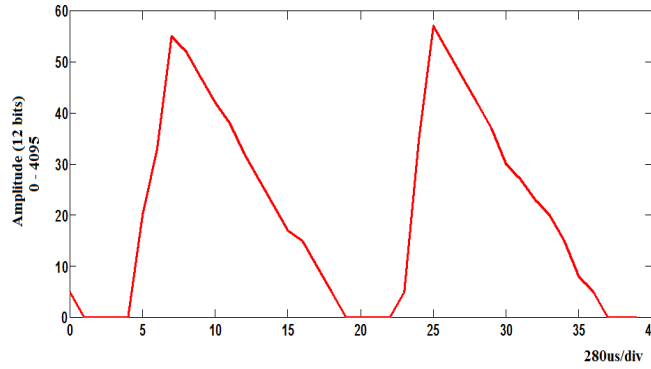
Fig. 12 shows the captured digital signals using $F28335$ DSP controller. These digital signals are similar to the ones in Fig. 10. The 12 bits magnitude seen in the waveforms ($2^{12} = 4096$) can be easily convert into its analog values by using the same conversion ratio as the sensors and offset values.



(i)



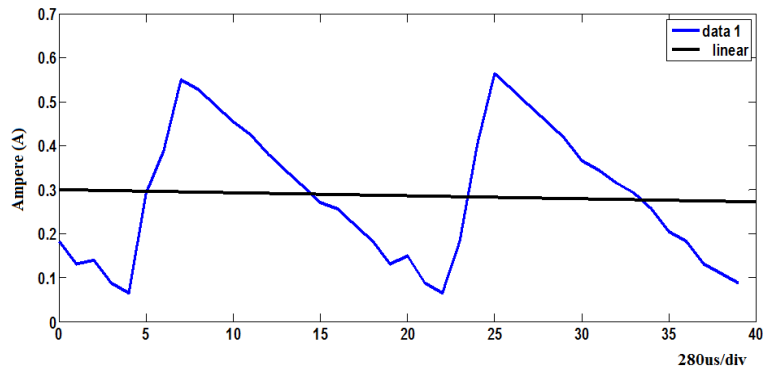
(ii)



(iii)

Fig. 12. Hardware results of phase inductor L_4 . (i) Phase inductor voltage V_{L4} (ii) Series current measuring (iii) Conventional RC sensing.

As mention in the methodology, the proposed method requires the phase inductor voltage to convert into phase inductor current. Hence, the information seen in Fig. 12(i) is fed into the proposed algorithm to produce the phase inductor current. Fig. 13 shows the normalized phase inductor current i_{L4} for all the sensing technique.



(i)

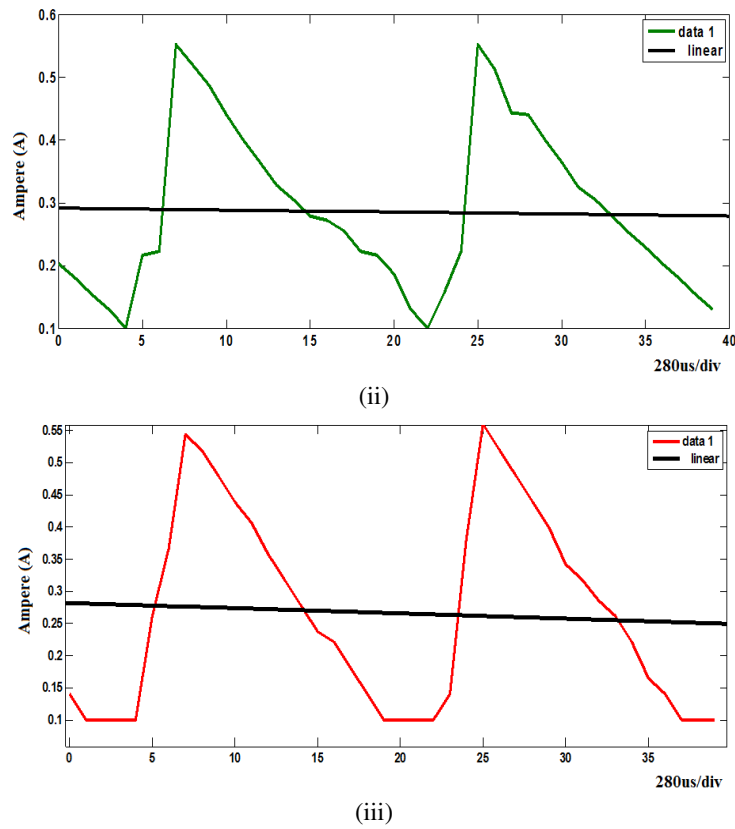


Fig. 13. Normalized phase inductor current i_{L4} . (i) Proposed technique (ii) Series current measuring (iii) Conventional RC sensing.

From the normalized output seen in Fig. 13(i), the proposed method waveform is similar to the series current and conventional RC filter technique. Fig. 13 also shows that the mean value of phase inductor L_4 is currently at 0.3A output. From this experiment, the hardware results are seen to be similar compared to the simulation results. Fig. 14 shows a comparison between the proposed sensing technique, conventional technique, and the series current sensing technique. It is obviously shown that the proposed method has an additional stage in which digital RC is placed before the normalized control block. It is, however, offers both lossless I^2R and reduced components in measuring the inductor current as compared to conventional RC filter and series current sensing technique.

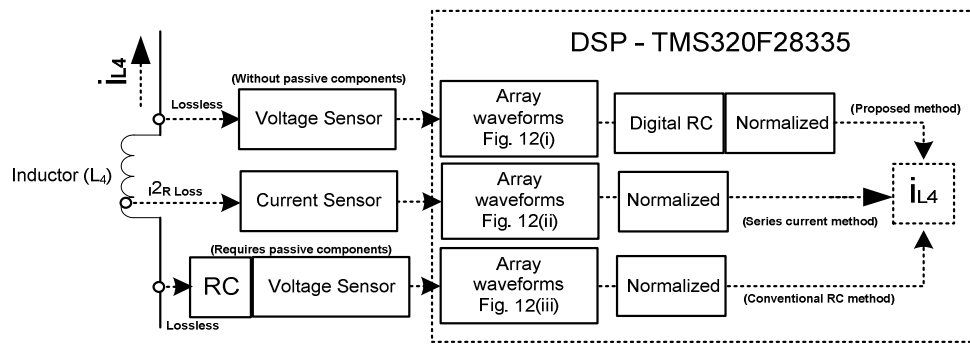


Fig. 14. Comparison of the control blocks.

6. Conclusion

This paper has proposed a current-less technique in measuring the phase inductor current by using a digital RC network. This method eliminates the needs of having additional components and can be applied to integrated circuits. The comparisons of digital RC network as compared to the conventional RC network and series current sensing techniques have been carried out. The proposed method is able to convert the high-frequency voltage measured from the phase inductor and transform the values into the phase inductor current without any delay or difficulty. By comparing the signals of proposed method to the conventional RC filter and series current sensing techniques, the waveforms of both signals are similar. However, the proposed method is able to improve the efficiency of the converter and at the same time offers reduced components.

Acknowledgment

The author gratefully acknowledge the support of The Sumitomo Foundation, Japan for the fundings. We were also grateful to our partners from Universiti Tenaga Nasional (Centre of Electrical Transportation system) for their valuable suggestions and assistance in this project.

References

- [1] G. Beccuti, M. Kvasnica, G. Papafotiou, and M. Morari, A Decentralized Explicit Predictive Control Paradigm for Parallelized DC-DC Circuits, *IEEE Transactions On Control Systems Technology*, Vol. 21, No. 1, 2013.
- [2] P. Cheng, M. Vasic, O. Garcia, J. A. Oliver, P. Alou, and J. A. Cobos, Minimum Time Control for Multiphase Buck Converter: Analysis and Application, *IEEE Trans. On Power Electronics*, Vol. 29, No. 2, 2014.
- [3] R. G. Retegui, M. Benedetti, M. Funes, P. Antoszezuk, and D. Carrica, Current Control for High-Dynamic High-Power Multiphase Buck Converter, *IEEE Trans. On Power Electronics*, Vol. 27, No. 2, 2012.
- [4] S. Abe, M. Shoyama, and T. Ninomiya, Optimal Design of Output Filter Capacitor for Peak Current Mode Control Converter with First-Order Response, *IEEE Trans. Power Electronics and Applications*, 13th European Conference, 2009.
- [5] K. Siri, C. Q. Lee, T. F. Wu, Current Distribution Control For Parallel Connected Converters: Part I, *IEEE Trans.* 1992.
- [6] Jiann-Jong Chen, Ming-Xiang Lu, Tse-Hsu Wu, Yuh Shyan Hwang, Sub-1-V Fast-Response Hysteresis-Controlled CMOS Buck Converter Using Adaptive Ramp Techniques, *IEEE Transactions on (VLSI) Systems*, Vol. 21, Issue: 9, 2013.

- [7] J. A. F. Yahaya, Muhamad Mansor, Model Predictive Control for Current Balancing in a Four-Phase Buck Converter, *International Journal of Renewable Energy Research*, Vol. 6, No. 2, 2016.
- [8] W. Huang, A new control for multi-phase buck converter with fast transient response, in *Proc. Appl. Power Electron. Conf.*, 2001, pp. 273–279.
- [9] E. Dallago, M. Passoni, and G. Sassone, Lossless current sensing in low voltage high current DC/DC modular supplies, *IEEE Trans. Ind. Electron.*, vol. 47, no. 12, pp. 1249–1252, Dec. 2000.
- [10] Y. Zhang, R. Zane, A. Prodic, R. Erickson, and D. Maksimovic, Online calibration of MOSFET on-state resistance for precise current sensing, *IEEE Trans. Power Electron. Lett.*, vol. 2, no. 3, pp. 100–103, Sep. 2004.
- [11] W. Huang, G. Schuellein, and D. Clavette, A scalable multiphase buck converter with average current share bus, in *Proc. Appl. Power Electron. Conf.*, 2003, pp. 438–443.
- [12] Yong-Seong Roh, Young-Jin Moon, Jeongpyo Park, Min-Gyu Jeong, and Changsik Yoo, A Multiphase Synchronous Buck Converter With a Fully Integrated Current Balancing Scheme, *IEEE Trans. On Power Electronics*, Vol. 30, No. 9, Sept. 2015.
- [13] X. Zho and P. Xu, A Novel Current-Sharing Control Technique for Low-Voltage High-Current Voltage Regulator Module Applications, *IEEE Trans. Power Electronics*, vol. 15, pp. 1153-1162, Nov. 2000.
- [14] Pallab Midya, Philip T. Krein, Matthew F. Greuel, Sensorless Current Mode Control – An observer-Based Technique for DC-DC Converters, *IEEE Transaction on Power Electronics*, Vol. 16, No. 4, July, 2001.
- [15] Pallab Midya, Philip T. Krein, Closed-Loop Noise Properties of Pulse-Width Modulated Power Converters, *IEEE Transaction*, 1995.